NETWORKS AND HETEROGENEOUS MEDIA
©American Institute of Mathematical Sciences
Volume **6**, Number **3**, September **2011**

doi:10.3934/nhm.2011.6.425

pp. **425–442**

FORCE-BASED MODELS OF PEDESTRIAN DYNAMICS

Mohcine Chraibi and Ulrich Kemloh

Jülich Supercomputing Centre
Forschungszentrum Jülich
52425 Jülich, Germany

Andreas Schadschneider

Institute for Theoretical Physics
Universität zu Köln
50937 Köln, Germany

Armin Seyfried

Jülich Supercomputing Centre
Forschungszentrum Jülich
52425 Jülich, Germany
and
Department D, Division Civil Engineering
Bergische Universität Wuppertal
Pauluskirchstraße 7, 42285 Wuppertal, Germany

Abstract. Force-based models describe the interactions of pedestrians in terms of physical and social forces. We discuss some intrinsic problems of this approach, like penetration of particles, unrealistic oscillations and velocities as well as conceptual problems related to violations of Newton's laws. We then present the generalized centrifugal force model which solves some of these problems. Furthermore we discuss the problem of choosing a realistic driving force to an exit. We illustrate this problem by investigating the behaviour of pedestrians at bottlenecks.

1. **Introduction.** In the past several aspects of pedestrian dynamics were investigated e.g., analysis of design issues [29, 33], evacuation planning [56, 43, 54, 16, 38] and computer animation [51, 2, 37]. For further information we refer to [44, 9, 58, 27] and the reviews [39, 42, 57]. Of particular importance are empirical results which provide a benchmark test for any model and allow their calibration. This issue is discussed in more detail elsewhere in [41].

Models which are continuous in space can be classified in force-based models [13, 36, 30, 33, 60, 50, 5, 54, 52, 53, 29, 8], where the trajectories of pedestrians are defined by a system of differential equations, and rule-based models [55, 43, 1, 4, 2, 51, 37, 48], defined through set of rules describing the reaction of pedestrians to their surrounding.

Force-based models are very popular approach for modelling pedestrian dynamics which assumes that pedestrian's movement is a consequence of exterior forces acting

2000 *Mathematics Subject Classification.* Primary: 82C22, 97M99; Secondary: 990B20.
Key words and phrases. Pedestrian dynamics, flow, bottleneck, force-based models.

on pedestrians. In this paper we give an overview about the state of the art of force-based modelling of pedestrian dynamics and a brief analysis of this approach. We point out some difficulties and ways to overcome these problems.

Force-based models take Newton's second law of dynamics as a guiding principle. Given a pedestrian i with coordinates $\overrightarrow{R_i}$ one defines the set of all pedestrians that influence pedestrian i at a certain moment as $\mathcal{N}_i$ and the set of walls or boundaries that act on pedestrian i as $\mathcal{W}_i$. In general the forces defining the equation of motion are split into driving and repulsive forces. The repulsive forces model the collision-avoidance performed by pedestrians and should guarantee a certain volume exclusion for each pedestrian. The driving force, on the other hand, models the intention of a pedestrian to move to a certain destination and walk with a desired speed.

Formally the movement of each pedestrian is defined by the equation of motion

$$m_i \ddot{\overrightarrow{R_i}} = \overrightarrow{F_i} = \overrightarrow{F_i^{\mathrm{drv}}} + \sum_{j \in \mathcal{N}_i} \overrightarrow{F_{ij}^{\mathrm{rep}}} + \sum_{w \in \mathcal{W}_i} \overrightarrow{F_{iw}^{\mathrm{rep}}}\,, \tag{1}$$

where $\overrightarrow{F_{ij}^{\mathrm{rep}}}$ denotes the repulsive force from pedestrian j acting on pedestrian i, $\overrightarrow{F_{iw}^{\mathrm{rep}}}$ is the repulsive force emerging from the obstacle w and $\overrightarrow{F_i^{\mathrm{drv}}}$ is a driving force. m_i is the mass of pedestrian i.

Most of force-based models describe pedestrian dynamics qualitatively fairly well. Collective phenomena like lane formation [13, 12, 60], oscillations at bottlenecks [13, 12], the "faster-is-slower" effect [30, 35], clogging at exit doors [12, 60] are reproduced. Unfortunately there are only poor quantitative descriptions of these phenomena or in case of the "faster-is-slower" effect a convincing experimental evidence is still lacking.

For design and evacuation purposes a reliable quantitative investigation is essential. In order to provide an experimental basis for a quantitative model verification, several experiments under laboratory conditions were conducted, see [41] for a detailed discussion.

Force-based models contain free parameters that can be adequately calibrated to achieve a good quantitative description [22, 23, 29, 36, 18]. In most works quantitative investigations of pedestrian dynamics were restricted to a specific scenario or geometry, like one-dimensional motion [4, 50, 48], behaviour at bottlenecks [29, 20, 19], two-dimensional motion [36] or outflow from a room [25, 26, 24, 59]. In more complex scenarios e.g. a building where all "basic" geometries (corridors, bottlenecks, corners, ...) and their variants can be found, it becomes more challenging to calibrate a model that describes the dynamics in the complete building correctly.

Usually, implementations of the repulsive force require additional elements to guarantee realistic behaviour, especially in high density situations. Here strong overlapping of pedestrians [30, 60] or negative and high velocities [13, 33] occur as artefacts of the force-based description. This then has to be rectified by supplementing the equation of motion (1) with other procedures, e.g. collision detection algorithms. This increases the complexity of the model. Sometimes the additional procedures are not well documented which can lead to misinterpretation of the model. In [7] it was shown that algorithms for collision detection and avoidance can dominate the dynamics and mask the role of the repulsive force.

While the repulsive force was investigated intensively in the past [13, 30, 60, 53, 36, 5], the influence of the specific form of the driving force has so far not been paid

much attention. The standard form of this force is

$$\overrightarrow{F_i^{\mathrm{drv}}} = m_i \frac{\overrightarrow{v_i^0} - \overrightarrow{v_i}}{\tau}, \tag{2}$$

with a relaxation time τ and a certain desired velocity $\overrightarrow{v_i^0}$. Although the expression of Eq. (2) is simple, it is not clear how to choose the desired direction $\overrightarrow{e_i^0} = \frac{\overrightarrow{v_i^0}}{\|\overrightarrow{v_i^0}\|}$ in a given situation. In most works it is neglected where exactly $\overrightarrow{e_i^0}$ points and a straightforward solution like directing pedestrians to a single point leads to artificial jams in particular for wide bottlenecks or corners in large rooms. In [52] an Ansatz with directing lines was introduced to steer pedestrians around 90° and 180° corners. In [15] an algorithm for generating automatically a navigation graph in complex buildings in combination with directing lines at corners was proposed. Gloor et al [10] used a path-oriented approach to model the desired direction of agents with given hiking paths.

In this work we show on the basis of a force-based model the impact of the desired direction on the dynamics of a system by measuring the outflow from a bottleneck with different widths.

2. Force-based models.

These models are motivated by the observation that the motion of pedestrians deviates from a straight path in the presence of other pedestrians. Therefore their motion is accelerated which according to Newton's laws implies the existence of a force.

2.1. Social-force models.

The social force model (SFM) [13] was the first mathematical implementation of Lewin's idea [31] to explain behavioural changes of people by "social fields". The repulsive force is described by means of repulsive potential with elliptical equipotential lines. Although the repulsive force is symmetrical in space, i.e. pedestrians in front and behind exert the same force, and computationally very intensive (exponential function), the SFM reproduces several qualitative characteristics of pedestrian dynamics, e.g. the formation of lanes in counterflow. Nevertheless various improvements of the original SFM were suggested to overcome the problems encountered. In [14] a more realistic form of the forces was introduced which reflects the anisotropic character of the interactions. Furthermore this generalized SFM takes into account repulsive forces that emerge when pedestrians have physical contact or get too close to each other. Lakoba et al. [30] pointed out other problems like the unrealistic choice of parameters which e.g. leads to extreme physical forces of 6000 N. The problem of the parameter choice in the SFM was investigated in [23] by calibration based on an evolutionary optimization algorithm. Parisi et al. [36] investigated the difficulties of SFM concerning quantitative description of pedestrian dynamics by introducing the "respect mechanism". This rule-based mechanism helps to mitigate overlapping among pedestrians.

2.2. Centrifugal force model.

Yu et al. [60] proposed a new expression for the repulsive force which differs from the typical exponential repulsive function in the SFM and its variants. The centrifugal force model (CFM) considers both the headway $\overrightarrow{R_{ij}}$ and the relative velocity v_{ij} among pedestrians in the specification of the force:

$$\overrightarrow{F_{ij}^{\mathrm{rep}}} \propto f(v_{ij}, \| \overrightarrow{R_{ij}} \|^{-1}) \cdot \frac{\overrightarrow{R_{ij}}}{\| \overrightarrow{R_{ij}} \|}. \tag{3}$$

Compared to the SFM, the repulsive force in the CFM reflects several new ideas. Besides the simple form of Eq. (3), the force is anisotropic since its range of influence is reduced to range of vision of pedestrians, which is 180°. This is realized by a proper choice of the function f. Furthermore it takes into account the influence of the relative velocity, i.e. faster pedestrians in front of a slower pedestrians do not affect his/her movement.

The CFM is one of the first models that describes clearly "collision detection technique" to deal with the problem of overlapping pedestrians and succeed in managing collisions among pedestrians, which can be interpreted as a failure of the avoidance-mechanism expressed in form of repulsive forces.

3. Problems of force-based models.

As mentioned earlier the force-based modelling approach of pedestrian dynamics is based on Newtonian dynamics. Paradoxically some principles of the latter are conceptual problems of force-based models. The first problem is Newton's third law. According to this principle two particles interact by forces of equal magnitudes and opposite directions. For pedestrians this law is unrealistic since e.g. normally a pedestrian does not react to pedestrians behind him/her. Even if the angle of vision is taken into account, the forces mutually exerted on each other are not of the same magnitude[1] so that the "actio=reactio"-principle does not hold in pedestrian dynamics.

The second problem emerges from the assumption that the forces acting on a pedestrian are additive. According to the superposition principle the total force acting on a particle is given by the sum of the individual forces. This can lead to undesired effects when modelling pedestrian dynamics, especially in dense situations where unrealistic backwards movement or high velocities can occur. This problem becomes more serious with increasing interaction range of the forces.

Further problems are related to the Newtonian equation of motion describing particles with inertia. This could leads to overlapping and oscillations of the modelled pedestrians. Depending on the strength of the repulsive forces the geometrical form modelling pedestrians body can be excessively overlapped and violate the principle of volume exclusion. Small overlaps could in principle be acceptable and be interpreted as "elastic deformations" of the body. However, large overlaps or even inter-penetrations are clearly unrealistic. Oscillations occur in force-based models because pedestrians do not stop and keep moving independently of the actual situation. In some situations pedestrians perform repetitive backwards and forwards movement due to e.g. high repulsive forces. In real situations pedestrians stop when they evaluate the situation as blocked or change the direction.

Avoiding overlapping between pedestrians and oscillations in their trajectories is difficult to accomplish in force-based models. On one hand, increasing the strength of the repulsive force with the aim of excluding overlapping during simulations leads to oscillations in the trajectories of pedestrians. Consequently backward movements occur which is not realistic especially in evacuation scenarios. On the other hand, reducing the strength of the repulsive force (to avoid oscillations) leads inevitably to overlapping between pedestrians or between pedestrians and obstacles.

In order to quantify the dual problem of overlapping and oscillations during simulations we introduce two quantities. First, we define an overlapping-proportion

[1] An extreme case would be stalking where even the sign of the interactions is different!

by

$$o^{(v)} = \frac{1}{n_{ov}} \sum_{t=0}^{t_{\text{end}}} \sum_{i=1}^{N} \sum_{j>i}^{N} o_{ij}\,, \tag{4}$$

with

$$o_{ij} = \frac{A_{ij}}{\min(A_i, A_j)} \leq 1, \tag{5}$$

where N is the number of simulated pedestrians and t_{end} the duration of the simulation. A_{ij} is the overlapping area of the circles i and j with areas A_i and A_j, respectively. n_{ov} is the cardinality of the set

$$\mathcal{O} := \{o_{ij} : o_{ij} \neq 0\}\,. \tag{6}$$

For $n_{ov} = 0$, $o^{(v)}$ is set to zero. For the sake of convenience we assumed that pedestrians are represented with circles.

For a pedestrian with velocity $\overrightarrow{v_i}$ and desired velocity $\overrightarrow{v_i^0}$ we define the oscillation-proportion as

$$o^{(s)} = \frac{1}{n_{os}} \sum_{t=0}^{t_{\text{end}}} \sum_{i=1}^{N} S_i\,, \tag{7}$$

where S_i quantifies the oscillation-strength of pedestrian i and is defined as follows:

$$S_i = \frac{1}{2}(-s_i + |s_i|)\,, \tag{8}$$

with

$$s_i = \frac{\overrightarrow{v_i} \cdot \overrightarrow{v_i}^0}{\| \overrightarrow{v_i^0} \|^2}\,, \tag{9}$$

and n_{os} is the cardinality of the set

$$\mathcal{S} := \{s_i : s_i \neq 0\}. \tag{10}$$

Here again $o^{(s)}$ is set to zero if $n_{os} = 0$. The proportions $o^{(v)}$ and $o^{(s)}$ are normalized to 1 and describe the evolution of the overlapping and oscillations during a simulation.

Increasing the strength of the repulsive force to make pedestrians "impenetrable" leads to a decrease of the overlapping-proportion $o^{(v)}$. Meanwhile, the oscillation-proportion $o^{(s)}$ increases, thus the system tends to become unstable. Large values of the oscillation-proportion $o^{(s)}$ imply less stability. For $s_i = 1$ one has $\overrightarrow{v_i} = -\overrightarrow{v_i}^0$, i.e. a pedestrian moves backwards with desired velocity. Even values of s_i higher than 1 are not excluded and can occur during a simulation.

Unfortunately, it is difficult to adjust the strength of the repulsive force in order to get an overlapping-free model which is at the same time also oscillation-free.

4. **Generalized centrifugal force model.** Pedestrians are not just point-like particles influenced by force fields of other point-like particles. Instead they should be treated as extended objects which change their shape with speed [48, 50].

The generalized centrifugal force model (GCFM) [5] offers a more detailed description by modelling pedestrians as ellipses with velocity-dependent semi-axes. It takes into account the distance between the "edges" of the pedestrians as well as their relative velocities. An elliptical volume exclusion has several advantages over a circular one. First, a circle is symmetric with respect to its center. This contradicts the fact that pedestrians need more space in their direction of motion than transverse to it. Second, the situation in front, i.e. in the direction of motion, is

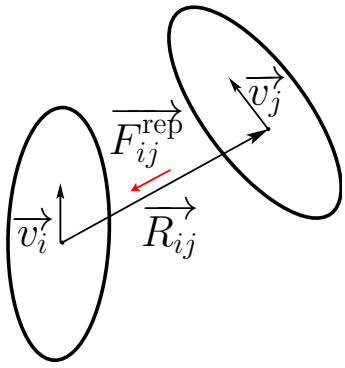

FIGURE 1. Direction of the repulsive force.

more relevant than that behind. That implies that the influence of persons directly in front is much stronger. This asymmetrical force behaviour is better reflected by ellipses rather than circles.

The movement of pedestrians is a direct result of superposition of repulsive and driving forces acting on the center of each pedestrian. Repulsive forces are acting on pedestrian i from other pedestrians in their neighbourhood and eventually from e.g. walls and stairs to prevent collisions and overlapping (see Fig. 1). The driving force (2), however, adds a positive term to the resulting force, to enable movement of pedestrian i in a certain direction with a given desired speed $\| \overrightarrow{v_i^0} \|$.

Given the direction connecting the positions of pedestrians i and j:

$$\overrightarrow{R_{ij}} = \overrightarrow{R_j} - \overrightarrow{R_i}, \qquad \overrightarrow{e_{ij}} = \frac{\overrightarrow{R_{ij}}}{\| \overrightarrow{R_{ij}} \|} \tag{11}$$

The repulsive force then reads

$$\overrightarrow{F_{ij}^{\text{rep}}} = -m_i k_{ij} \frac{(\eta {v_i}^0 + v_{ij})^2}{\text{dist}_{ij}} \overrightarrow{e_{ij}}, \tag{12}$$

with

$$\text{dist}_{ij} = \| \overrightarrow{R_{ij}} \| - r_i(v_i) - r_j(v_j) \tag{13}$$

the effective distance between pedestrian i and j and r_i the polar radius of pedestrian i.

This definition of the repulsive force in the GCFM reflects several aspects. First, the force between two pedestrians decreases with increasing distance. In the GCFM it is inversely proportional to their distance (13). Furthermore, the repulsive force takes into account the relative velocity v_{ij} between pedestrian i and pedestrian j. The following special definition ensures that slower pedestrians are less affected by the presence of faster pedestrians in front of them:

$$\begin{aligned} v_{ij} &= \frac{1}{2}[(\overrightarrow{v_i} - \overrightarrow{v_j}) \cdot \overrightarrow{e_{ij}} + |(\overrightarrow{v_i} - \overrightarrow{v_j}) \cdot \overrightarrow{e_{ij}}|] \\ &= \begin{cases} (\overrightarrow{v_i} - \overrightarrow{v_j}) \cdot \overrightarrow{e_{ij}} & \text{if } (\overrightarrow{v_i} - \overrightarrow{v_j}) \cdot \overrightarrow{e_{ij}} > 0 \\ 0 & \text{otherwise.} \end{cases} \end{aligned} \tag{14}$$

As in general pedestrians react only to obstacles and pedestrians that are within their perception, the reaction field of the repulsive force is reduced to the angle of

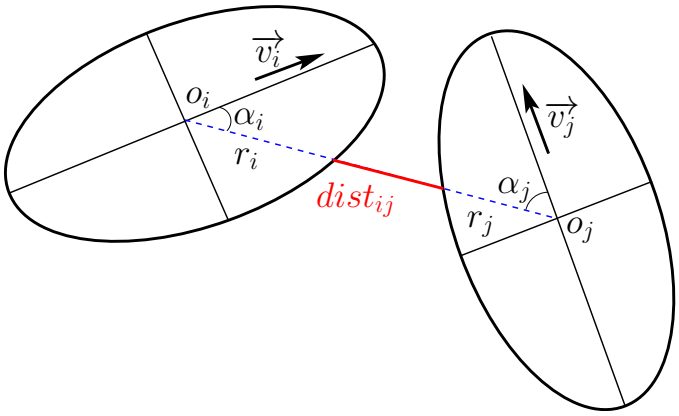

FIGURE 2. dist_{ij} is the distance between the borders of the ellipses i and j along a line connecting their centres.

vision (180°) of each pedestrian, by introducing the coefficient

$$\begin{aligned} k_{ij} &= \frac{1}{2}\frac{\overrightarrow{v_i}\cdot\overrightarrow{e_{ij}} + |\,\overrightarrow{v_i}\cdot\overrightarrow{e_{ij}}\,|}{v_i} \\ &= \begin{cases} (\overrightarrow{v_i}\cdot\overrightarrow{e_{ij}})/\parallel\overrightarrow{v_i}\parallel & \text{if } \overrightarrow{v_i}\cdot\overrightarrow{e_{ij}} > 0 \quad \& \quad \parallel\overrightarrow{v_i}\parallel \neq 0 \\ 0 & \text{otherwise.} \end{cases} \end{aligned} \tag{15}$$

The coefficient k_{ij} is maximal when pedestrian j is in the direction of movement of pedestrian i and minimal when the angle between j and i is bigger than 90°. Thus the strength of the repulsive force depends on the angle.

4.1. **Distance between ellipses.** In the following we give details for the calculation of the distance dist_{ij} between two ellipses which is defined as the distance between the borders of the ellipses, along a line connecting their centres (Fig. 2).

By proper choice of the coordinate system the ellipse i may be written as quadratic form,

$$\frac{x^2}{a_i^2} + \frac{y^2}{b_i^2} = 1\,. \tag{16}$$

In polar coordinates, with the origin at the center of the ellipse and with the angular coordinate α_i measured from the major axis, one gets

$$x = r_i\cos(\alpha_i)\,, \qquad y = r_i\sin(\alpha_i)\,. \tag{17}$$

By replacing the expressions of x and y in Eq. (16) and rearranging, we obtain the expression

$$qr_i^2 - 1 = 0, \tag{18}$$

for the polar radius r_i with

$$q = \frac{\cos^2\alpha_i}{a_i^2} + \frac{\sin^2\alpha_i}{b_i^2}. \tag{19}$$

In the same manner, we determine the polar radius r_j.

Finally, the distance dist_{ij} is determined as follows (Fig. 2):

$$\mathrm{dist}_{ij} = \parallel\overrightarrow{o_io_j}\parallel - r_i - r_j\,. \tag{20}$$

Remark 1. Note that the distance between two ellipses can be non-zero even when the ellipses touch or overlap. Therefore the forces are generically different from those between circles, even for the same configuration.

5. **Distance of closest approach.** As the repulsive force (12) depends inversely on the distance between two pedestrians, it becomes maximal when two pedestrians are in contact. As a consequence of the anisotropy of ellipses the contact distance is in general not zero. In following we give a definition of this distance.

Definition 5.1. The distance of closest approach (DCA) of two ellipses is the smallest distance between their borders, along a line connecting their centres while they are not overlapping (see Fig. 3 top).

To mitigate overlapping the repulsive forces are high for distances in a certain neighbourhood of the distance of closest approach, see $\tilde{l}$ in Fig. 4. An analytical solution of this distance for two arbitrary ellipses is presented in [62].

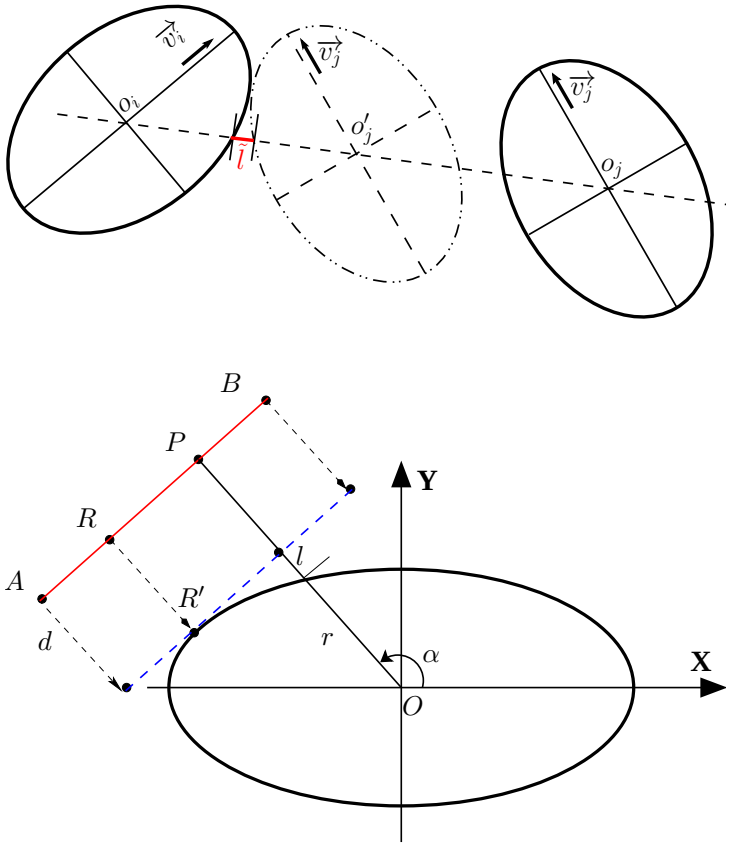

FIGURE 3. Top: Distance of closest approach of two ellipses. Bottom: Distance of closest approach between an ellipse and a line.

5.1. **Distance of Closest Approach of an Ellipse to a Line Segment.** Similarly to the definition of the distance of closest approach for two arbitrary ellipses [62] we define the DCA for an arbitrary ellipse and a line segment. This distance is important to calculate the repulsive force between a pedestrian and a wall as defined in Eq. (12).

Notation. For two points A and B [AB] denotes the line segments delimited with A and B while (AB) denotes the line joining A and B.

Let E be an ellipse with semi-axis a and b and a segment line [AB]. We assume without loss of generality that E is in canonical position (center at origin of the coordinate system O and its major and minor semi-axis are parallel to the X-axis and the Y-axis). See Fig. 3 bottom.

Problem. *Given E and [AB] find the DCA* l

From Fig. 3 bottom one can see that

$$l = \| \overrightarrow{OP} \| - r - d \tag{21}$$

P is the nearest point on [AB] to O (see the notes of P. Bourke [3]).

Knowing α we can easily calculate r. To solve Eq. (21) one has to find the quantity d, which would be the necessary amount to translate [AB] along the direction of $\overrightarrow{OP}$ such that it becomes tangential to the ellipse.

Let R' be the translation of R. Then

$$x_{R'} = x_R - d \cdot \cos(\alpha); \qquad y_{R'} = y_R - d \cdot \sin(\alpha) \tag{22}$$

The parametric definition of the line segment [AB] is

$$x = x_A + u \cdot (x_B - x_A); \quad y = y_A + u \cdot (y_B - y_A); \qquad (u \in [0,\ 1]) \tag{23}$$

$x_{R'} \in$ ellipse implies

$$\frac{{x'_R}^2}{a^2} + \frac{{y'_R}^2}{b^2} = 1 \tag{24}$$

Or,

$$\frac{(x_R - d \cdot \cos(\alpha))^2}{a^2} + \frac{(y_R - d \cdot \sin(\alpha))^2}{b^2} = 1 \tag{25}$$

rearranging Eq. (25) to make d the subject yields the quadratic equation

$$p \cdot d^2 + q \cdot d + s = 0 \tag{26}$$

with

$$p = \frac{\cos(\alpha)^2}{a^2} + \frac{\sin(\alpha)^2}{b^2} > 0 \tag{27}$$

$$q = -2 \cdot \left(\frac{x_R \cdot \cos(\alpha)}{a^2} + \frac{y_R \cdot \sin(\alpha)}{b^2} \right) \tag{28}$$

$$s = \frac{x_R^2}{a^2} + \frac{y_R^2}{b^2} - 1 \tag{29}$$

If the point R is known then the solution of the problem is

$$d = \frac{-q - \sqrt{\Delta}}{2 \cdot p} \tag{30}$$

with Δ the discriminant of Eq. (26):

$$\Delta = q^2 - 4 \cdot p \cdot s \tag{31}$$

As in general R is not known, we rearrange Eq. (25) to make u the subject and become

$$p_1 \cdot u^2 + q_1 \cdot u + s_1 = 0 \tag{32}$$

with

$$p_1 = \frac{x_{BA}^2}{a^2} + \frac{y_{BA}^2}{b^2} \geq 0 \tag{33}$$

$$q_1 = 2 \cdot \left(\frac{x_A - d \cdot \cos(\alpha)}{a^2} \cdot x_{BA} + \frac{y_A - d \cdot \sin(\alpha)}{b^2} \cdot y_{BA} \right) \tag{34}$$

$$s_1 = \frac{(x_A - d \cdot \cos(\alpha))^2}{a^2} + \frac{(y_A - d \cdot \sin(\alpha))^2}{b^2} - 1 \tag{35}$$

with the substitutions $x_{BA} = x_B - x_A$ and $y_{BA} = y_B - y_A$.

Since the line (AB) is tangential to the ellipse, Eq. (32) has only one solution. Therefore the discriminant is zero:

$$\Delta = q_1^2 - 4 \cdot p_1 \cdot s_1 = 0, \tag{36}$$

which leads to

$${q_1}^2 = 4 \cdot p_1 \cdot s_1 \tag{37}$$

Supposing that O, P, A and B are not collinear we solve Eq. (37) and get

$$d_{1,2} = \frac{\pm a \cdot b \cdot \sqrt{p_1} - x_{BA} \cdot y_B + y_{BA} \cdot x_A}{y_{BA} \cdot \cos(\alpha) - x_{BA} \cdot \sin(\alpha)} \tag{38}$$

and

$$d = \min(|d_1|, |d_2|). \tag{39}$$

For the calculated value of d we find u:

$$u = \frac{-q_1}{2 \cdot p_1} \tag{40}$$

and check the inequality:

$$0 \leq u \leq 1\,. \tag{41}$$

If the inequality (41) does not hold or O, P, A and B are collinear then R is an end point of [AB], i.e. A or B. In this case we solve Eq. (30) twice for A and B and get d_A and d_B.

Finally the solution is

$$d = \min(|d_A|, |d_B|). \tag{42}$$

6. **Simulation.** The initial value problem in Eq. (1) was solved using an Euler scheme with fixed-step size $\Delta t = 0.01$ s. First the state variables of all pedestrians are determined. Then the update to the next step is performed. Thus, the update in each step is parallel.

In order to reduce the range of the repulsive force and to avoid infinite values by zero distances we implement a two-sided Hermite-interpolation of the repulsive force. The interpolation guarantees that the norm of the repulsive force decreases smoothly to zero for $\text{dist}_{ij} \to r_c^-$ and $r_c = 2$ m. For $\text{dist}_{ij} \to \tilde{l}^+$ the interpolation avoids an increase of the force to infinity but to $f_m = 3 \cdot \parallel \overrightarrow{F_{ij}^{\text{rep}}}(r_{\text{eps}}) \parallel$ at $s_0 = r_{\text{eps}}$ and $r_{\text{eps}} = 0.1$ m, where it remains constant. $\tilde{l}$ is defined in Def. 5.1. Fig. 4 shows the dependence of the repulsive force on the distance for constant relative velocity.

The right interpolation function P_r and the left one P_l (dashed parts of the function in Fig. 4) are defined using

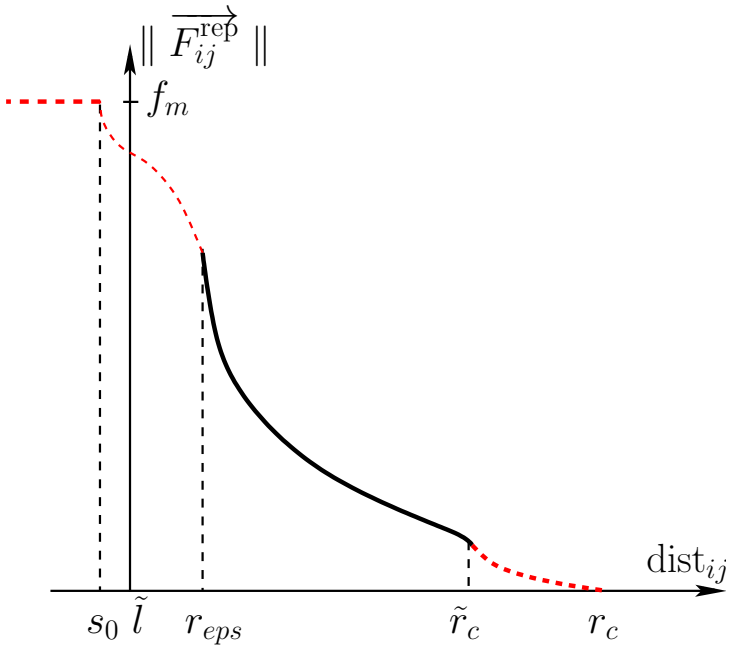

FIGURE 4. The interpolation of the repulsive force between pedestrians i and j Eq. (12) depending on dist_{ij} and the distance of closest approach $\tilde{l}$, see Eq. 13 and Def. 5.1. As the repulsive force also depends on the relative velocity v_{ij}, this figure depicts the curve of the force for $v_{ij} = \text{const}$. The left and right dashed curves are defined in Eqs. (44) and (43) respectively. The wall-pedestrian interaction has an analogous form.

$$\begin{aligned} P_r(\tilde{r}_c) &= \| \overrightarrow{F_{ij}^{\text{rep}}}(\tilde{r}_c) \|, \qquad P_r(r_c) = 0 \\ (P_r)'(\tilde{r}_c) &= \| \left(\overrightarrow{F_{ij}^{\text{rep}}}(\tilde{r}_c) \right)' \|, \qquad (P_r)'(r_c) = 0 \end{aligned} \tag{43}$$

with $\tilde{r}_c = r_c - r_{\text{eps}}$ and

$$\begin{aligned} P_l(s_0) &= f_m, \qquad P_l(r_{\text{eps}}) = \| \overrightarrow{F_{ij}^{\text{rep}}}(r_{\text{eps}}) \| \\ (P_l)'(s_0^+) &= 1, \qquad (P_l)'(r_{\text{eps}}) = \| \left(\overrightarrow{F_{ij}^{\text{rep}}}(r_{\text{eps}}) \right)' \| \ . \end{aligned} \tag{44}$$

where the prime indicates the derivative. s_0 is the minimum allowed magnitude of the effective distance of two ellipses.

Remark 2. Due to the superposition of the forces the inequality:

$$\text{dist}_{ij} \geq s_0 \tag{45}$$

for pedestrians i and j is not guaranteed.

Simulations with the GCFM yield the right relation between velocity and density both in single-file movement and wide corridors with one set of parameters [5]. In this section we investigate instead the influence of the desired direction. By means

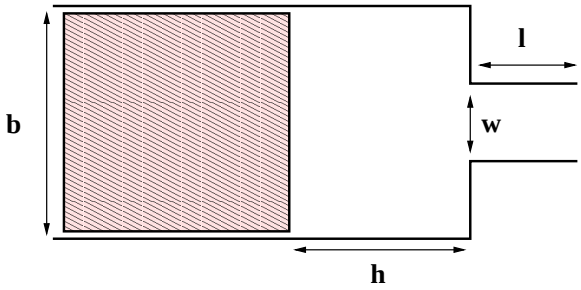

FIGURE 5. Scenario set-up. Pedestrians move from a holding area (shaded area) through the bottleneck. $l = 2\,\mathrm{m}$, $h = 4.5\,\mathrm{m}$ and $b = 4\,\mathrm{m}$.

of the flow through a bottleneck we show that different strategies lead to significant differences in the dynamics of the system.

The desired speeds of pedestrians are Gaussian distributed with mean $\mu = 1.34$ m/s and standard deviation $\sigma = 0.26$ m/s. The time constant τ in the driving force Eq. (2) is set to 0.5 s, i.e. $\tau \gg \Delta t$. For simplicity, the mass m_i is set to unity. We set the strength parameter of the repulsive force η to 0.2. We have performed several simulations with $N = 60$ pedestrians, see Fig 5. The width of the bottleneck is varied from 0.8 m to 1.2 m in steps of 0.1 m. Then from 1.2 m to 2.5 m in steps of 0.2 m. The flow through the bottleneck is calculated at a line directly after passing the bottleneck as following

$$J = \frac{N-1}{t_{\text{last}} - t_{\text{first}}} \tag{46}$$

with t_{first} the passing time of the first pedestrian and t_{last} the passing time of the last one.

We tested two different direction choice strategies. In the first strategy (strategy 0) the desired direction of each pedestrian points to the middle of the bottleneck. In the second strategy (strategy 1) the desired direction of a pedestrian is parallel to the walls of the corridor. Only near a bottleneck, when the pedestrian can not "see" its exit, it is directed towards the center of the entrance (Fig. 6).

Fig. 7 shows the simulation results for both strategies. For small width of the bottleneck the flow is slightly invariant with respect to the directing strategies. For bigger widths a clear discrepancy in the results is observed. In accordance with the empirical data the flow increases with the width if strategy 1 is used. For strategy 0 and $w > 1\,\mathrm{m}$ the flow shows no dependence of the width and stagnates. The modelled pedestrians do not take advantage of the full width of the bottleneck, unlike in strategy 1.

Remark 3. While the SFM fails to solve without any side effects the duality problem overlapping-oscillations, with the set of parameter chosen for this simulation the GCFM shows a good balance between oscillations (Eq. 7) and overlapping (Eq .4). Meanwhile it delivers a good quantitative description of pedestrian dynamics. See [5] for further details.

7. **Visualisation.** Visualisation plays a key role in the development of models. The main advantage of visualisation methods is their ability to communicate large amounts of information in a short time period, recall the saying "one picture is

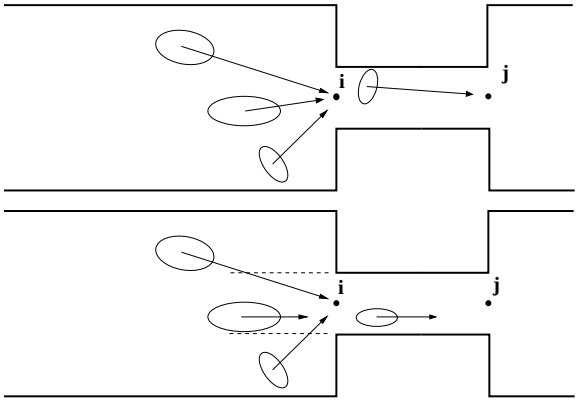

FIGURE 6. Top: Strategy 0. All pedestrians are directed exactly towards the middle of the exit i and j. Bottom: Strategy 1. Depending on their position pedestrians adapt their direction. In the range where the exit of the bottleneck is visible (marked with dashed lines) the direction is longitudinal. Outside this area they are directed towards the middle of the bottleneck.

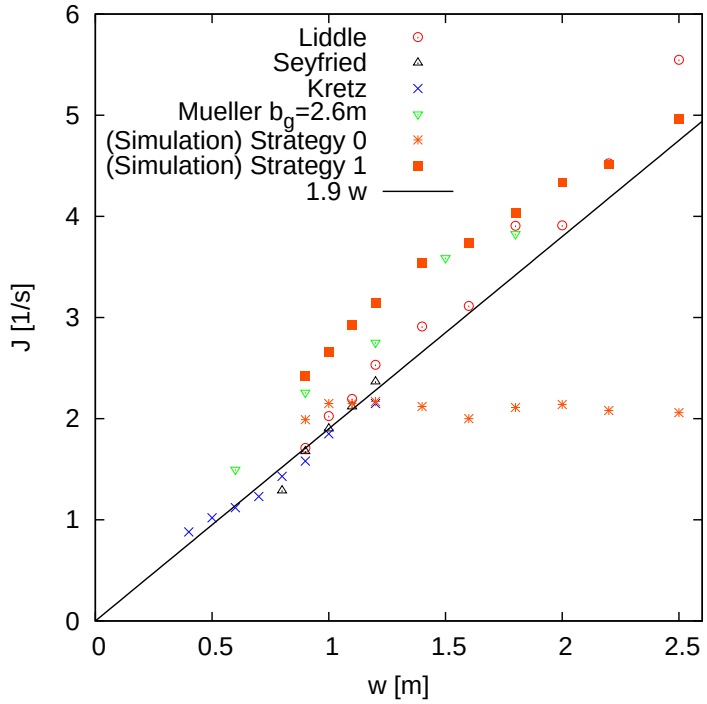

FIGURE 7. Flow through a bottleneck with different widths in comparison with empirical data Liddle [32], Seyfried [47], Kretz [28] and Mueller[34]. For strategy 0 the flow increases slightly for small widths, then it stagnates independently of the width.

worth a thousand words". There is no better, quick and simple way to assess a model than a snapshot of the results. However, depending on the information one is interested in, a single snapshot might be insufficient. In the field of pedestrian dynamics, just like in many other fields, an animation of the whole simulation is often required to properly assess the dynamics of the system. Visualisation is thus often used as the first primary validation technique and eases the calibration of the model.

Several problems of force-based models that we discussed in Sec. 3 can be detected by a good visualisation of the trajectories produced by a simulation. Problems like wrong sorting of pedestrians at a door or the dynamic torque shown by the ellipses become visible. Individual pedestrians can easily be tracked and other issues like unrealistic blocking between individual pedestrians in a jam situation can be visually analysed. Another aspect is visual control of the qualitative aspect of pedestrian dynamics produced by the model, e.g. lanes formation or clogging at exits. Some examples of the problems described in Sec. 3 are shown in Fig. 8. Extreme values of η (0.1 and 0.7) lead to strong overlapping among pedestrians and oscillations.

For visualisation purposes, we developed the Trajectories Visualisation Tool (TraVisTo), which is released under GNU General Public Licence (GPL) [11] and is built on top of the Visualisation Toolkit (VTK) libraries [45]. VTK is open source and platform independent library for computer graphic and provides many algorithms for visualisation and data analysis as well as an interface to the C++, Java, Python and Tcl languages. TraVisTo reads a file containing the simulation results (coordinates, velocities, orientations, ...) together with geometry information and allows the user to interact with this information in form of an animation, for instance focusing on an area of interest or masking views. TraVisTo can also be used in an online mode, where simulation results are directly streamed to the application.

Visualisation thus makes it possible to assess problems which are not considered in measurements or which cannot directly be measured. While a good visualisation is indispensable to control the qualitative aspect of pedestrian dynamics and to eliminate anomalies that emerge from an inappropriate choice of forces, it is not possible to judge through the quantitative ability of the model. The other side of the coin is the fact that a visualisation can look realistic but quantitatively far away from being correct. For example an overlapping-free or oscillation-free simulation that shows e.g. several collective phenomena does not imply that the model yields the correct density-velocity relation.

8. **Conclusions.**

Force-based models have successfully been applied for the description of pedestrian and crowd dynamics. However, this approach has some intrinsic problems, like the occurrence of oscillations or penetration of the particles representing pedestrians. We have discussed the origin of these problems and suggested solutions in form of the generalized centrifugal force model combined with an accurate modelling of the 2-D projection of the human body by means of ellipses with velocity dependent semi-axes. Thereby the varying space requirement of pedestrian while in motion is adequately modelled.

Furthermore, we showed with help of two different strategies that modelling the desired direction of pedestrians is important and influences deeply the dynamics of the system. This suggests that the direction choice in the driving force has to be more investigated.

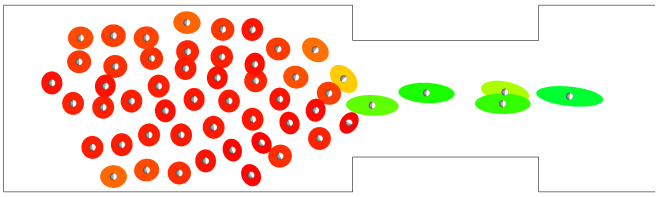

(a) Blocking of pedestrians at the bottleneck when using strategy 0. The bottleneck width is not effectively used. Screenshot taken at t=20 seconds.

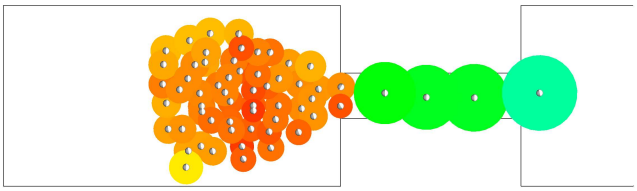

(b) Strong overlapping between pedestrians ($\eta = 0.1$) due to weak repulsive forces. Screenshot taken at t=9 seconds.

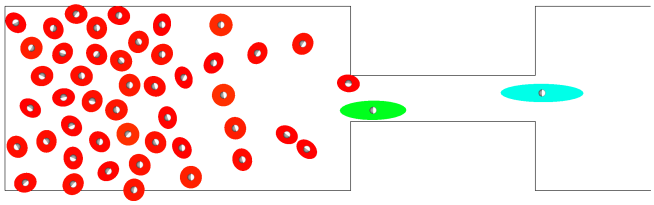

(c) Oscillations between pedestrians ($\eta = 0.7$), strong repulsive forces cause some pedestrians to perform backwards movement (Note the orientation of the pedestrians in the rear of the bottleneck). In addition some pedestrians have overcome the wall forces and passed through the walls due to these extreme forces. Screenshot taken at $t = 9$ s.

FIGURE 8. Blocking, overlapping and oscillations between pedestrians. The simulation is performed with 60 pedestrians. The colour and shapes of the ellipses are correlated to their instant velocity. Slow ellipses are red.

Acknowledgments. This work is within the framework of two projects. The authors are grateful to the Deutsche Forschungsgemeinschaft (DFG) for funding the project under Grant-Nr.: SE 1789/1-1 as well as the Federal Ministry of Education and Research (BMBF) for funding the project under Grant-Nr.: 13N9952 and 13N9960.

REFERENCES

[1] M. Asano, T. Iryo and M. Kuwahara, *Microscopic pedestrian simulation model combined with a tactical model for route choice behaviour*, Transportation Research Part C: Emerging Technologies, **18** (2010), 842–855.

[2] J. V. Berg, M. Lin and D. Manocha, *Reciprocal velocity obstacles for real-time multi-agent navigation*, in "Robotics and Automation," IEEE International Conference on Robotics and Automation Pasadena, CA, USA, 2008.

[3] P. Bourke, *Minimum distance between a point and a line*, accessed 24, December 2010. Available from: `http://paulbourke.net/geometry/pointline/`.

[4] M. Chraibi and A. Seyfried, *Pedestrian dynamics with event-driven simulation*, in [27], 713–718.

[5] M. Chraibi, A. Seyfried and A. Schadschneider, *Generalized centrifugal force model for pedestrian dynamics*, Phys. Rev. E, **82** (2010), 046111.

[6] M. Chraibi, A. Seyfried, A. Schadschneider and W. Mackens, "Quantitative Description of Pedestrian Dynamics with a Force-Based Model," IEEE/WIC/ACM International Joint Conference on Web Intelligence and Intelligent Agent Technology, **3**, IEEE Computer Society, Los Alamitos, CA, USA, (2009), 583–586.

[7] M. Chraibi, A. Seyfried, A. Schadschneider and W. Mackens, "Quantitative Verification of a Force-Based Model for Pedestrian Dynamics," Traffic and Granular Flow '09, 2009.

[8] Z. Fang, J. P. Yuan, Y. C. Wang and S. M. Lo, *Survey of pedestrian movement and development of a crowd dynamics model*, Fire Safety Journal, **43** (2008), 459–465.

[9] E. R. Galea, ed., "Pedestrian and Evacuation Dynamics 2003," CMS Press, London, 2003.

[10] C. Gloor, L. Mauron and K. A. Nagel, "Pedestrian Simulation for Hiking in the Alps," Proceedings of Swiss Transport Research Conference (STRC), Monte Verita, 2003.

[11] GNU General public license, `http://www.gnu.org/licenses/gpl.html`.

[12] D. Helbing, *Collective phenomena and states in traffic and self-driven many-particle systems*, Computational Materials Science, **30** (2004), 180–187.

[13] D. Helbing and P. Molnár, *Social force model for pedestrian dynamics*, Phys. Rev. E, **51** (1995), 4282–4286.

[14] D. Helbing, I. J. Farkas, P. Molnár and T. Viscek, *Simulation of pedestrian crowds in normal and evacuation situations*, in [44], 21–58.

[15] M. Höcker, V. Berkhahn, A. Kneidl, A. Borrmann and W. Klein, "Graph-based Approaches for Simulating Pedestrian Dynamics in Building Models," 8^{th} European Conference on Product & Process Modelling (ECPPM), University College Cork, Cork, Ireland, 2010.

[16] S. Holl and A. Seyfried, *Hermes - an evacuation assistant for mass events*, inSiDe, **7** (2009), 60–61.

[17] S. P. Hoogendoorn, "Walking Behavior in Bottlenecks and its Implications for Capacity," TRB 2004 Annual Meeting, 2004.

[18] S. P. Hoogendoorn and W. Daamen, *A novel calibration approach of microscopic pedestrian models*, in "Pedestrian Behavior" (ed. H. Timmermans), Emerald, 2009, p. 195.

[19] S. P. Hoogendoorn and W. Daamen, *Pedestrian behavior at bottlenecks*, Transportation Science, **39** (2005), 147–159.

[20] S. P. Hoogendoorn, W. Daamen and P. H. L Bovy, "Extracting Microscopic Pedestrian Characteristics from Video Data," TRB 2004 Annual Meeting Washington DC: National Academy Press, 2003.

[21] S. P. Hoogendoorn, W. Daamen and P. H. L. Bovy, *Microscopic pedestrian traffic data collection and analysis by walking experiments: Behaviour at bottlenecks*, in [9], 89–100.

[22] S. P. Hoogendoorn, W. Daamen and R. Landman, *Microscopic calibration and validation of pedestrian models - Cross-comparison of models using experimental data*, in [58], 253.

[23] A. Johansson, D. Helbing and P. K. Shukla, *Specification of the social force pedestrian model by evolutionary adjustment to video tracking data*, Advances in Complex Systems, **10** (2007), 271–288.

[24] A. Kirchner, "Modellierung und Statistische Physik biologischer und sozialer Systeme," Ph.D thesis, Universität zu Köln, Germany, 2003.

[25] A. Kirchner and A. Schadschneider, *Simulation of evacuation processes using a bionics-inspired cellular automaton model for pedestrian dynamics*, Physica A, **312** (2002), 260–276.

[26] A. Kirchner, K. Nishinari and A. Schadschneider, *Friction effects and clogging in a cellular automaton model for pedestrian dynamics*, Phys. Rev. E, **67** (2003), 056122.

[27] W. Klingsch, C. Rogsch, A. Schadschneider and M. Schreckenberg, eds., "Pedestrian and Evacuation Dynamics 2008," Springer-Verlag, Berlin, Heidelberg, 2010.
[28] T. Kretz, A. Grünebohm and M. Schreckenberg, *Experimental study of pedestrian flow through a bottleneck*, J. Stat. Mech., **10** (2006), P10014.
[29] T. Kretz, S. Hengst and P. Vortisch, *Pedestrian flow at bottlenecks - validation and calibration of Vissim's social force model of pedestrian traffic and its empirical foundations*, in "International Symposium of Transport Simulation" (ed. M Sarvi), Monash University, Melbourne, Australia, 2008.
[30] T. I. Lakoba, D. J. Kaup and N. M. Finkelstein, *Modifications of the Helbing-Molnár-Farkas-Vicsek social force model for pedestrian evolution*, Simulation, **81** (2005), 339–352.
[31] K. Lewin, "Field Theory in Social Science," Greenwood Press Publishers, 1951.
[32] J. Liddle, A. Seyfried, T. Rupprecht, W. Klingsch, A. Schadschneider and A. Winkens, "An Experimental Study of Pedestrian Congestions: Influence of Bottleneck Width and Length," Traffic and Granular Flow '09, 2009, arXiv:0911.4350.
[33] R. Löhner, *On the modelling of pedestrian motion*, Applied Mathematical Modelling, **34** (2010), 366–382.
[34] K. Müller, "Zur Gestaltung und Bemessung von Fluchtwegen für die Evakuierung von Personen aus Bauwerken auf der Grundlage von Modellversuchen," Ph.D thesis, Magdeburg, Germany, 1981.
[35] D. R. Parisi and C. O. Dorso, *Morphological and dynamical aspects of the room evacuation process*, Physica A, **385** (2007), 343–355.
[36] D. R. Parisi, M. Gilman and H. Moldovan, *A modification of the social force model can reproduce experimental data of pedestrian flows in normal conditions*, Physica A, **388** (2009), 3600–3608.
[37] J. Ondřej, J. Pettré, A. Olivier and S. Donikian, "A Synthetic-Vision-Based Steering Approach for Crowd Simulation," SIGGRAPH '10: ACM SIGGRAPH, 2010.
[38] A. Schadschneider, *I'm a football fan ... get me out of here*, Physics World, **21**, July 2010.
[39] A. Schadschneider, W. Klingsch, H. Klüpfel, T. Kretz, C. Rogsch and A. Seyfried, *Evacuation dynamics: Empirical results, modeling and applications*, Encyclopedia of Complexity and System Science, 2009, 3142.
[40] A. Schadschneider, H. Klüpfel, T. Kretz, C. Rogsch and A. Seyfried, *Fundamentals of pedestrian and evacuation dynamics*, in "Multi-Agent Systems for Traffic and Transportation Engineering" (eds. Ana Bazzan and Franziska Klügl), IGI Global, Hershey, Pennsylvania, USA, 2009, chapter 6, 124–154.
[41] A. Schadschneider and A. Seyfried, *Empirical results for pedestrian dynamics and their implications for modelling*, Networks and Heterogeneous Media, **3** (2011), 545–560
[42] A. Schadschneider and A. Seyfried, "Modeling Pedestrian Dynamics - From Experiment to Theory and Back," Traffic and Granular Flow '09, 2009.
[43] V. Schneider and R. Könnecke. *Simulating evacuation processes with ASERI*, in [44], 303–314.
[44] M. Schreckenberg and S. D. Sharma, eds., "Pedestrian and Evacuation Dynamics 2001," Springer, 2002.
[45] W. Schroeder, K. Martin and B. Lorense, "Visualization Toolkit: An Object-Oriented Approach to 3D Graphics," 4^{th} edition, Kitware Inc., 2006.
[46] A. Seyfried, M. Boltes, J. Kähler, W. Klingsch, A. Portz, T. Rupprecht, A. Schadschneider, B. Steffen and A. Winkens, *Enhanced empirical data for the fundamental diagram and the flow through bottlenecks*, in [27], 145.
[47] A. Seyfried, O. Passon, B. Steffen, M. Boltes, T. Rupprecht and W. Klingsch, *New insights into pedestrian flow through bottlenecks*, Transportation Science, **43** (2009), 395–406.
[48] A. Seyfried, A. Portz and A. Schadschneider, *Phase coexistence in congested states of pedestrian dynamics cellular automata*, in "Cellular Automata" (eds. S. Bandini, S. Manzoni, H. Umeo and G. Vizzari), LNCS 6350, Springer, 2010, 496–505, arXiv:1006.3546.
[49] A. Seyfried and A. Schadschneider, *Validation of cellular automata models of pedestrian dynamics using controlled large-scale experiments*, Cybernetics and Systems, **40** (2009), 367.
[50] A. Seyfried, B. Steffen and T. Lippert, *Basics of modelling the pedestrian flow*, Physica A, **368** (2006), 232–238.
[51] W. Shao and D. Terzopoulos, *Autonomous pedestrians*, in "Eurographics/ACM SIGGRAPH Symposium on Computer Animation" (eds. K. Anjyo and P. Faloutsos), 2005.
[52] B. Steffen and A. Seyfried, *Modelling of pedestrian movement around* 90° *and* 180° *bends*, in "First International Conference on Soft Computing Technology in Civil" (eds. B. H. V.

Topping and Y. Tsompanakis), Structural and environmental engineering, Civil-Comp Press, Stirlingshire, UK, 2009.
[53] B. Steffen and A. Seyfried, *The repulsive force in continous space models of pedestrian movement*, arXiv:0803.1319v1, 2008.
[54] A. Steiner, M. Philipp and A. Schmid, "Parameter Estimation for a Pedestrian Simulation Model," Swiss Transport Research Conference, 2007.
[55] P. A. Thompson and E. W. Marchant, *A computer model for the evacuation of large building populations*, Fire Safety Journal, **24** (1995), 131–148.
[56] P. A. Thompson and E. W. Marchant, *Testing and application of the computer model 'SIMULEX'*, Fire Safety Journal, **24** (1995), 149–166.
[57] H. Timmermans, ed., "Pedestrian Behavior," Emerald, 2009.
[58] N. Waldau, P. Gattermann, H. Knoflacher and M. Schreckenberg, eds., "Pedestrian and Evacuation Dynamics 2005," Springer, 2007.
[59] D. Yanagisawa, A. Kimura, A. Tomoeda, N. Ryosuke, Y. Suma, Kazumichi Ohtsuka and Katsuhiro Nishinari, *Introduction of frictional and turning function for pedestrian outflow with an obstacle*, Phys. Rev. E, **80** (2009), 036110.
[60] W. J. Yu, L. Y. Chen, R. Dong and S. Q. Dai, *Centrifugal force model for pedestrian dynamics*, Phys. Rev. E, **72** (2005), 026112.
[61] X. Liu, W. Song and J. Zhang, *Extraction and quantitative analysis of microscopic evacuation characteristics based on digital image processing*, Physica A, **388** (2009), 2717–2726.
[62] X. Zheng and P. Palffy-Muhoray, *Distance of closest approach of two arbitrary hard ellipses in two dimensions*, Phys. Rev. E, **75** (2007), 061709.

Received December 2010; revised May 2011.

E-mail address: m.chraibi@fz-juelich.de
E-mail address: u.kemloh@fz-juelich.de
E-mail address: as@thp.uni-koeln.de
E-mail address: a.seyfried@fz-juelich.de